Nanosecond pulsed electric field delivery to biological samples : difficulties and potential solutions

Aude Silve[1,2], Julien Villemejane[1,2,3], Vanessa Joubert[1,2], Antoni Ivorra[1,2] and Lluis M. Mir[1,2]*

[1] CNRS, UMR 8121, Institut Gustave-Roussy, Villejuif, France.
[2] Univ Paris-Sud, UMR 8121.
[3] CNRS, SATIE, Institut d'Alembert, ENS Cachan, Cachan, France
* Corresponding author
UMR 8121 CNRS, Institut Gustave-Roussy, 39 r. C. Desmoulins, F-94805 Villejuif, France
Tél: + 33 1 42 11 47 92; Fax: + 33 1 42 11 52 45; mail: luismir@igr.fr

Keywords : nanosecond electric pulses, transmission line, waves propagation, impedance matching, electrochemical reactions, thermal effects, monitoring, breakdown of dielectric materials
Abbreviations: nsPEF: nanosecond pulsed electric field.

Summary
In this chapter we discuss particular features of the nanosecond electric pulsed fields (nsPEFs) that must be taken into account when experimenting on their delivery to biological samples. The purpose of the chapter is to provide future users of this technology with some advice on how to correctly apply it. It is first analyzed how propagation related phenomena can impact on the actual electric field pulse that is applied to the sample. In particular, it is shown that impedance matching for the exposure chamber will be a key element. It is then proposed to employ monitoring systems for voltage and current signals and some indications about their use and limitations are given. Finally, the electrochemical and thermal consequences of nsPEFs delivery are also discussed. We conclude that only excellent experimental conditions can result in robust, controlled and reproducible data on the nsPEFs biological effects.

Tip to the reader:
Non-bold italic symbols are employed here to denote scalars or time variables (e.g. a voltage signal in the time domain will be noted as $V(t)$ or V). Bold italic symbols are employed for complex variables (e.g. the Fourier Transform of a voltage signal $V(t)$ will be noted as $\boldsymbol{V}(\omega)$ or $\boldsymbol{V}$). On the other hand, bold non-italic symbols are employed for vectors such as the electric field, **E**, and the current density, **J**.

Draft version prepared by authors, the original can be found in chapter 18 of "Advanced Electroporation Techniques in Biology and Medicine" Editors: Andrei G. Pakhomov, Damijan Miklavcic and Marko S. Markov, CRC Press, 2010, ISBN: 9781439819067

Introduction

Electroporation using microsecond- or millisecond-long electric pulses is a well–known technology frequently used on the bench (e.g. bacteria and eukaryotic cells transformation in research laboratories) as well as at the bed (e.g. tumor treatment by electrochemotherapy, nowadays routinely used in Europe). NsPEF is an emerging technology that encompasses a lot of promises because it opens new opportunities for cell "electromanipulation". Indeed, with "long" (μs and ms) pulses, changes can only be generated at the level of the cell membrane, while "short" (ns) pulses can also provoke modifications at the level of the internal membranes. So, coming from the experience on the use of "long" pulses, several groups have started to use "short" pulses on living cells. It is also expected that, in the future, when equipment will become easier to use and accessible, many other groups will also apply this technology.

In this chapter we discuss particular features of nsPEFs delivery systems that must be taken into account when cells or tissues are exposed to the pulses. While the transition from the use of millisecond pulses to the delivery of microsecond pulses (and *vice versa*) is almost straightforward, the same cannot be said for the transition from the micro-/milli-second pulses to nsPEFs. The purpose of the present chapter is to provide future users of this technology with some advice on how to apply it correctly. More precisely, the ultimate goal of the chapter is to give a warning message regarding the use of nsPEF technology: usage of this technology is not straightforward; the experimental setup has to be designed carefully and some non-trivial considerations must be taken into account for ensuring experimental repeatability and reproducibility.

1. Taking propagation into account when applying nsPEFs

Generally, in bench-top sized electrical systems involving signals with frequencies below 1 MHz, or with durations longer than 1 μs, propagation related phenomena through the electrical connections can be considered negligible and it can be assumed that all points in a good electrical conductor reach the same voltage simultaneously. This is for example the case of conventional electroporation in which square pulses with a duration longer than 1 μs (typically 100 μs or longer) are applied. However, for nsPEFs the duration of the signals may be shorter that the time of propagation through the connections and, as a result, propagation related phenomena will be very relevant. Actually, as it will be shown here, even in the case of the long pulses employed in conventional electroporation it is possible to notice the consequences of propagation related phenomena.

In this section, we give a brief introduction to propagation related phenomena and we point out how these phenomena can be relevant when performing experiments involving nsPEFs. More comprehensive explanations for propagation related phenomena and concepts can be found in appropriate textbooks.

1.1 When propagation is relevant

A pair of long conductors separated by a dielectric forms a *transmission line* which is a structure that allows the transmission of voltage signals between two points. In a lot of cases such transmission appears to be instantaneous (e.g. switching on lights) but in others the voltage *wave* requires a significant amount of time to propagate from one point to the other one (e.g. wired electrical telegraphy). When transmission can be considered to be instantaneous, then each conductor of the transmission line is simply modeled as an ideal wire, which implies that all points along that wire have the same voltage value at the same time and that simple circuit theory is applicable (i.e. Kirchhoff's circuit laws). On the other hand, when propagation is relevant, then different phenomena associated to propagation are

manifested (e.g. delay, reflections and stationary waves) and the ideal wire model is no longer valid.

It is not always obvious to determine when propagation will be relevant or not. A continuous sinusoidal signal applied to one of the extremes of the transmission line will cause a sinusoidal pattern of voltages along the transmission line length as the signal propagates. The distance between the crests of this spatial sinusoidal pattern, measured in meters, is known as *wavelength*, λ, and it depends on the frequency of the excitation signal, f, expressed in hertz [Hz], and the propagation speed of the transmission line for that specific frequency, v, expressed in [$m.s^{-1}$]:

$$\lambda = \frac{v}{f}$$

Following this definition, in most textbooks it is stated that propagation phenomena have to be considered when the transmission line length, L, is larger than the wavelength of the signal in that particular line. This rule is not applicable for the case of pulse signals but, with some limitations, it can be transposed for those cases by saying: propagation related phenomena will have to be considered when the transmission line is longer than the wavelength corresponding to the maximum frequency at which the power spectral density of the pulse signal is still significant. For instance, in figure 1 it can be observed that the power spectral density of a 10 ns quasi-square pulse is still significant up to frequencies above 200 MHz and then, since for this 200 MHz frequency the wavelength will be in the order of 1 meter ($v \sim 2\times10^8$ m/s), according to the transposed rule it can be said that propagation phenomena have to be considered in benchtop sized systems. The frequency contents of a pulse signal will depend both on its duration (observe that in figure 1 the first notch corresponds to the inverse of pulse duration) and on its rising time: the steeper the voltage rise is, the broader the frequency content will be.

Intuitively, it could be thought that an alternative, and simpler, rule for deciding when propagation will be relevant in the case of pulse signals could be the following: propagation has to be taken into account when the propagation time of the pulse through the length of the transmission line is longer, or in the same order, than the duration of the pulse (i.e. propagation is relevant when $(L/v)>T$, where T is the duration of the pulse). However, as it will be shown now, this rule is not valid.

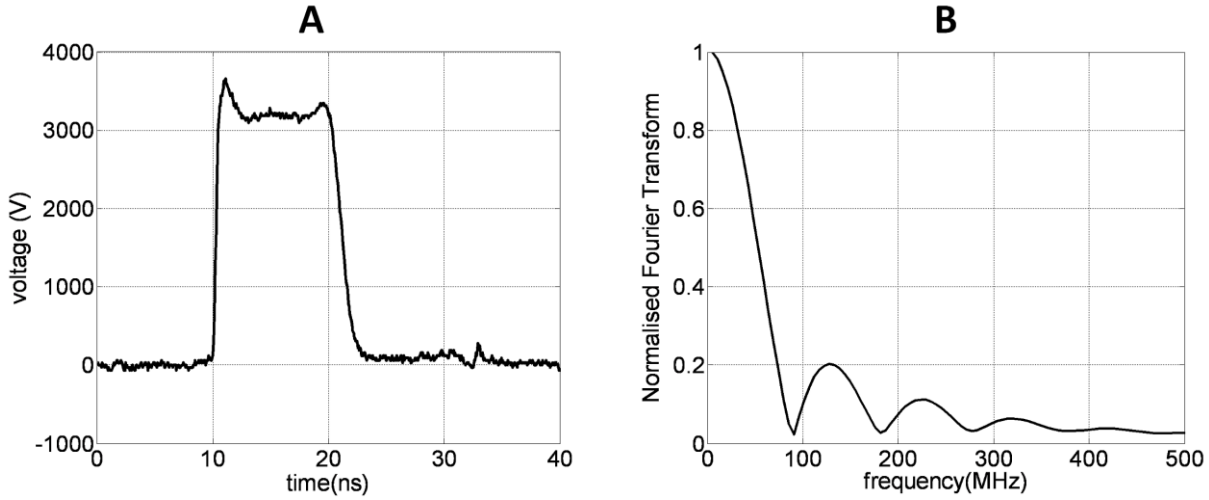

Fig 1 – Example of a 10-ns pulse delivered by a high-voltage pulse generator. A : voltage signal measured at a 50 Ω load, B : normalized spectrum of the voltage signal in A computed by performing the Fourier Transform.

As it has been mentioned, in conventional electroporation, propagation related phenomena are generally neglected. This is not surprising when it is taken into consideration that cables between the electrodes and the generator are shorter than one or two meters and that propagation speeds are in the order of 2×10^8 m.s^{-1}; it would take 10 ns for an electrical signal to travel along two meters of cable, which is negligible compared to the total duration of the pulse (i.e. $(L/v) << T$).

Nevertheless, it must be noted that the impact of propagation related phenomena on pulse signals with a duration larger than 1 µs can actually be noticed if careful observations are performed. For instance, figure 2 shows the result of a simulation in which a 100 µs pulse is delivered to a 10 Ω resistance through a cable with a propagation delay of 7.5 ns (equivalent to 1.5 meters). At first glance, it can be observed that the voltage signals at the generator (V_{in}) and at the load (V_{out}) are apparently identical. However, if the attention is focused on the pulse edges then it can be noticed that both signals are not strictly identical; V_{out} appears to be delayed and "softened". This distortion is not only due to mere propagation but also to a propagation related phenomena that is later described: signal reflections occur at the connections between the three different elements of the system (generator, cable and resistance).

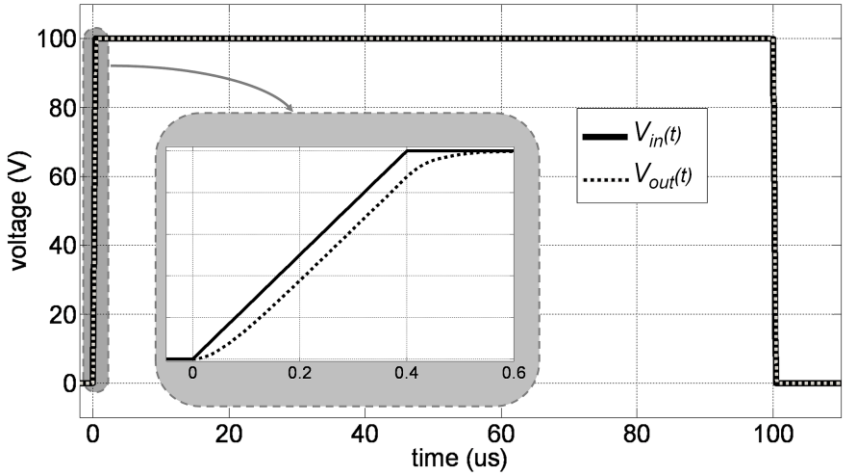

Fig 2 – Simulated example of the influence of propagation related phenomena on the shape of a 100 µs pulse. This is a SPICE simulation (LTspice IV by Linear Technology Corp.) in which the voltage at a 10 Ω load (V_{out}) was monitored when pulses (V_{in}) from a 0 Ω output impedance generator were delivered through a transmission line with propagation delay of 7.5 ns (equivalent to 1.5 m) and a characteristic impedance of 50 Ω (these concepts are later explained in section 1.2).

Therefore, propagation related phenomena actually do have an impact on the signals typically used in conventional electroporation. However, this impact is only significant on the pulse edges and, in terms of biological consequences, it has been demonstrated that the shape of those edges is not relevant in conventional electroporation (Kotnik *et al* 2001a).

1.2 Behavior of a transmission line

1.2.1 Propagation phenomenon

This section presents a classical electrical model for transmission lines (e.g. a coaxial cables) that reveals the propagation phenomenon.

For the whole length of the transmission line, the model consists of a succession of small electric sub-circuits each of which has a infinitesimal length, *dx*, very small compared to the wavelength. Because of their short length, in each sub-circuit it is possible to ignore the propagation phenomenon and then simple circuit theory analysis can be applied. Each sub-circuit (figure 3) is modeled by a series inductance ($L = l.dx$ [H], l is the linear inductance

[H.m^{-1}]) and a parallel capacitance ($C = c.dx$ [F], c is the linear capacitance [F.m^{-1}]). In addition, more complete models include resistive elements (a series resistance with L and a parallel conductance with C) which are responsible for an attenuation of propagated signals. Nevertheless, signal attenuation, and hence those dissipative elements, are usually neglected if the transmission line length does not exceed the wavelength by several orders of magnitude, which is the case in nsPEF experimental setups.

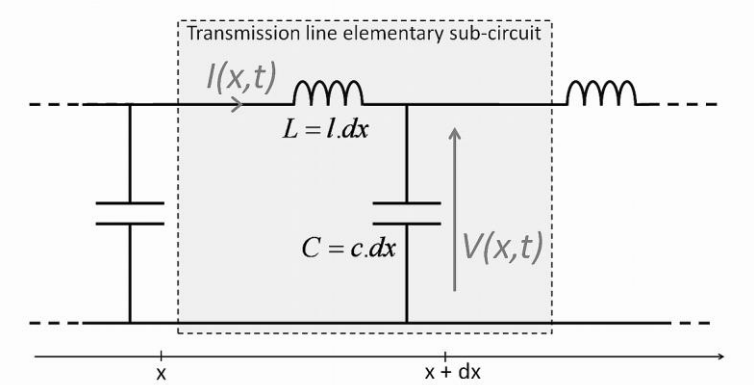

Fig 3- A transmission line can be modeled as a succession of elementary sub-circuits in which the propagation phenomenon can be neglected.

Then, despite the fact that each sub-circuit does not model the propagation phenomenon, it is possible to demonstrate by means of differential equations that voltage signals do propagate without distortion along the transmission line length (x) with an speed equal to :

$$v = \frac{1}{\sqrt{lc}} \qquad [\text{m/s}]$$

The propagation speed is fixed by the linear capacitance and inductance of the transmission line which are themselves imposed by the materials (especially the dielectric) that compose the line and by the geometry of the transmission line. In the case of a coaxial cable (presented on figure 4), approximate values for linear capacitance and inductance can be evaluated by the following expressions:

$$c = \frac{2\pi\varepsilon_0\varepsilon_r}{Log(\frac{r_1}{r_2})} \quad \left[\text{F.m}^{-1}\right] \quad and \quad l = \frac{\mu_0}{2\pi} Log(\frac{r_1}{r_2}) \quad \left[\text{H.m}^{-1}\right]$$

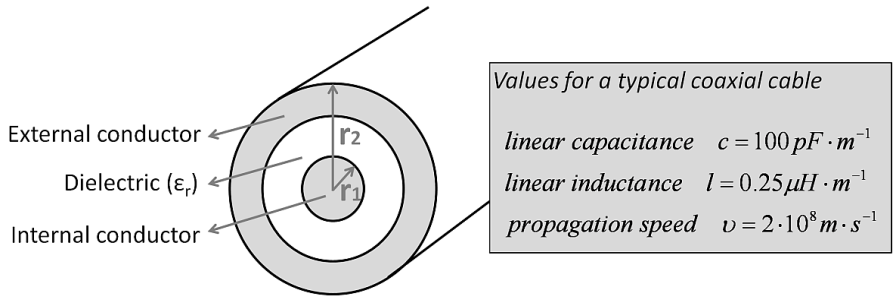

Fig 4- Electrical characteristics of a common coaxial cable.

1.2.2 Characteristic impedance and reflections

It can be demonstrated that at any point of the transmission line, when the signal propagates from the pulse generator to the biological load (+ direction), the voltage ($\boldsymbol{V}(x)_+$) and current ($\boldsymbol{I}(x)_+$) are related according to:

$$\frac{\boldsymbol{V}(x)_+}{\boldsymbol{I}(x)_+} = \boldsymbol{Z}_c \quad with \quad \boldsymbol{Z}_c = \sqrt{\frac{l}{c}}$$

The impedance introduced here, $\boldsymbol{Z}_c$, is called the *characteristic impedance* of the transmission line and is expressed in ohms. A standard value for radio-communications coaxial cables is 50 Ω.

The sample that is exposed to nsPEFs is commonly placed at the end of the cable and, from an electrical point of view, it can be modeled as a load with complex impedance $\boldsymbol{Z}$ (figure 5). If this load matches the characteristic impedance of the cable, i.e. when $\boldsymbol{Z}=\boldsymbol{Z}_c$, then the voltages and the currents at the two sides of transmission line termination (i.e. at the load and at the transmission line) are the same. In this case, all the energy that was propagating in the line is absorbed by the termination load. On the contrary, if $\boldsymbol{Z}\neq\boldsymbol{Z}_c$, a reflection will occur and a voltage wave will start to propagate in the opposite direction through the transmission line (i.e. from the load towards the pulse generator). This reflected wave is produced by the following mechanism: the Ohm's law is valid at both sides of the transmission line termination (i.e at the load and within the transmission line), therefore, since the voltage at both sides of the termination is also the same, when $\boldsymbol{Z}\neq\boldsymbol{Z}_c$ then it is required that a current is generated in the opposite direction in order to obey the Kirchhoff's current law. This current in turn generates the voltage wave ($\boldsymbol{V}(x)_- = \boldsymbol{Z}_c.\boldsymbol{I}(x)_-$). Once the reflected wave reaches the generator, another reflected wave (in the + direction) will be generated if the impedance of the generator (i.e. its output impedance) does not match the characteristic impedance.

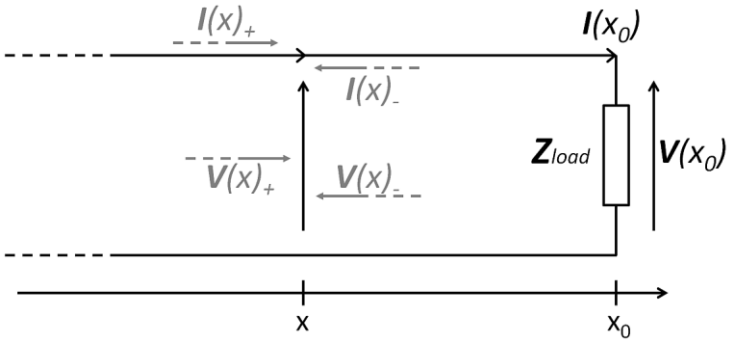

Fig 5 – Reflection on the termination of the transmission line. When the voltage and current signals propagating in the positive x-direction (V(x)+ ; I(x)+) reach a mismatched load, they are partially reflected. The reflected signals (V(x)- ; I(x)-) propagate in the opposite direction.

When reflections occur, part of the energy contained in the pulse is absorbed by the load and part of it is reflected. The fraction of energy transmitted to the load can be evaluated. Results of computation for a 50 Ω cable and a resistive termination R_{load}, are plotted on figure 6. As displayed, transmitted power is maximum for the impedance matching condition and it rapidly decreases for lower or larger load resistance values.

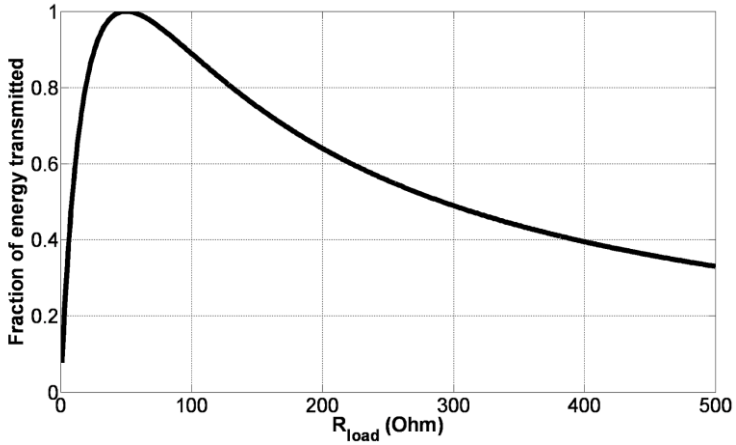

Fig 6 – Fraction of the energy transmitted to the load in the case of a resistive termination and a 50 Ω cable.

It is important to mention that not only the amount of energy transmitted to the load will be affected by reflection. Levels and shapes of voltage and current signals can be dramatically different from the ones initially coming out of the generator. Indeed, the voltage at the load and the current that runs through it are the sum of the initial signals and the reflected ones:

$$I(x_0) = I(x_0)_+ + I(x_0)_- \quad and \quad V(x_0) = V(x_0)_+ + V(x_0)_-$$

These relations are also true in the frequency domain:

$$\boldsymbol{I}(x_0) = \boldsymbol{I}(x_0)_+ + \boldsymbol{I}(x_0)_- \quad and \quad \boldsymbol{V}(x_0) = \boldsymbol{V}(x_0)_+ + \boldsymbol{V}(x_0)_-$$

The magnitudes and phases of the reflected signals can be expressed as functions of the initial signals defining the complex reflection coefficients $\boldsymbol{\Gamma}_V$ and $\boldsymbol{\Gamma}_I$.

$$\boldsymbol{\Gamma}_V = \frac{\boldsymbol{V}(x_0)_-}{\boldsymbol{V}(x_0)_+} = \frac{\boldsymbol{Z}_{load} - \boldsymbol{Z}_c}{\boldsymbol{Z}_{load} + \boldsymbol{Z}_c} \quad and \quad \boldsymbol{\Gamma}_I = \frac{\boldsymbol{I}(x_0)_-}{\boldsymbol{I}(x_0)_+} = \frac{\boldsymbol{Z}_c - \boldsymbol{Z}_{load}}{\boldsymbol{Z}_{load} + \boldsymbol{Z}_c} = -\boldsymbol{\Gamma}_V$$

Most striking examples of impedance mismatch are observable in extreme cases: a perfect short-circuit and a perfect open circuit. These examples are illustrated in figure 7. When the load is an open circuit, the voltage amplitude of the pulse at the load terminals is twice the amplitude of the pulse that was travelling from the generator. On the other hand, if the load is a short-circuit, the voltage amplitude at the load will be null.

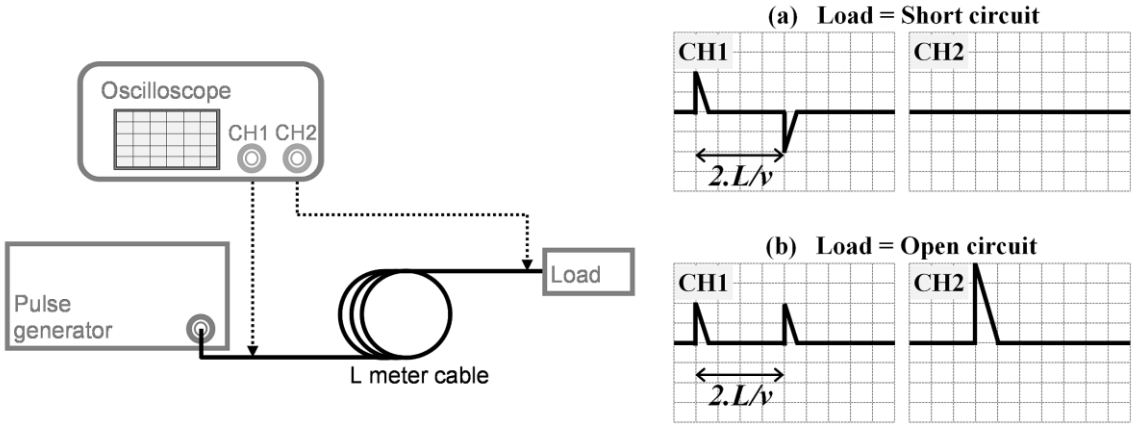

Fig 7 – Illustration of reflection for two different loads. A pulse generator is connected to a load through a transmission line (length L ; propagation speed v). If the load is a short circuit (a), the pulse is totally reflected in phase opposition and the resulting voltage on the load is null. If the load is an open circuit (b), the pulse is totally reflected in phase and the resulting voltage is twice the generated one.

As a consequence, it appears that for a given pulse generator and cable, the applied signals, and in particular the applied voltage, will be highly dependent on the impedance of the exposure device which in turn will depend on the properties of the biological sample.

1.3 Impedance matching for exposure devices

One of the common ways of doing *in-vitro* experiments is to use commercial electroporation cuvettes filled with cell suspensions (Garon *et al.* 2007, Kolb *et al.* 2006). Typical dimensions for such cuvettes are: an electrode area S of 1 cm^2 and an electrode separation l of 1 mm (volume = 0.1 ml). With these dimensions, a cuvette filled with a solution with a conductivity of σ = 1 S/m would have a resistance R ([Ω]) of approximately:

$$R = \frac{1}{\sigma} \cdot \frac{l}{S} = 10\ \Omega$$

If a 10 kV pulse was applied through a 50 Ω cable to such a cuvette, the resulting voltage according to the reflection coefficients would be 3.3 kV. In order to minimize such voltage drop, it is possible to adjust the conductivity of the solution or to modify the geometrical characteristics of the cuvette so that the load impedance is better matched to the characteristic impedance of the cable. Unfortunately, the experimental conditions narrow the degrees of freedom for such kind of solutions. For instance, although it is possible to reduce the conductivity of a cell suspension medium without altering its osmolarity by adding non-ionic agents (e.g. sucrose), the biological consequences of an extreme depletion of extracellular ions will add uncertainty to the interpretation of the observations.

Alternative solutions can be based on modifying the other elements of the system. For instance, it is possible to interconnect multiple generators in order to change the total source impedance or even to build an adapted generator (Hall *et al.* 2007). Another feasible solution is to insert a matching impedance in parallel with the load in those cases in which the sample has a high impedance. Some examples of this approach can be found for single cell exposure (Pakhomov *et al.* 2007). In this configuration most electrical power will be transmitted to the matching impedance and not directly to the biological sample.

In general, both, the resistive, R, and the reactive, X, components of the biological sample impedance ($\mathbf{Z} = R + jX$) will be significant at the frequencies of interest. Then, since the characteristic impedance of most transmission lines is purely resistive ($\mathbf{Z}_c$= 50 Ω + j0 Ω) some degree of pulse distortion will be almost unavoidable. In radio-communications it is possible to match reactive impedances by inserting compensating circuits. However, such compensating circuits are only useful for a single frequency or for a narrow bandwidth, which is not the case in pulse transmission.

Finally, it must be mentioned that the electrical connection from the transmission line to the sample will also contribute by itself to the global impedance of the load. Indeed, to connect a cuvette to a coaxial cable for *in vitro* experiments, a cuvette holder is necessary. Similarly, for performing *in vivo* experiments electrodes and connectors are necessary. These connections will basically add parasitic capacitances and inductances to the sample. An essential rule to limit parasitic effects is to make the connection as short as possible both to avoid propagation phenomena and to minimize inductive and capacitive parasitic elements.

In conclusion, even if all the issues described above are carefully addressed when implementing the experimental setup, distortion cannot be fully avoided. As a consequence, nsPEFs delivery must be accompanied by monitoring of the signal waveforms.

2. Breakdown of dielectric materials

The so-called *dielectric strength* of an electrically insulating material indicates the maximum electric field that the material can withstand without experiencing an abrupt failure of its insulating properties, either reversible or irreversible. Such failure in isolation is known

as *electrical breakdown* and it has been observed to occur in dielectric solids, gases and liquids. Dry air at atmospheric pressure has a dielectric strength of about 3 MV/m, polytetrafluoroethylene (Teflon^{TM}) has a dielectric strength higher than 60 MV/m, for alumina that value is about 13 MV/m, for polystyrene is about 20 MV/m and for fused silica it is possible to measure dielectric strength values above 400 MV/m. Breakdown process typically develops within a few nanoseconds (Beddow *et al.* 1966) and, for most materials, it is believed that the main phenomenon responsible for it is the *avalanche breakdown*: if the electric field is strong enough, free electrons in the dielectric material, either preexisting or freed by the electric field, are accelerated by the electric field and liberate additional electrons when colliding with the atoms of the material (i.e. ionization) so that the number of free charged particles is thus increased rapidly in an avalanche-like fashion. In the context of the present book, it is interesting to note that cell membrane electroporation is a case in which avalanche breakdown does not seem to be involved in the insulation failure process (Crowley 1973).

Transmission lines consist of metallic conductors and dielectrics. It is obvious then that the maximum voltage that a transmission line will be able to withstand will depend on the geometrical features of the line (e.g. the separation distance between conductors) and the dielectric strength of the dielectric material. A typical RG-58/U coaxial cable employed in 10BASE2 Ethernet computer networks and for radio-communications is specified to withstand 1500 V_{DC} between the inner conductor and the shield whereas a RG-194/U coaxial cable, intended for pulse transmission, can withstand DC voltages above 30 kV. Such increase in voltage tolerance comes with the drawback of a larger diameter (5 mm for the RG-58/U against 50 mm for the RG-194/U) and an increase of mechanical stiffness.

The same kind of considerations have to be applied to the connectors between the transmission lines and the exposure chamber or the pulse generator. Furthermore, an aspect that must be carefully taken into account is that the dielectric strength of air is particularly low (3 MV/m) and sparks (i.e. dielectric breakdown) may occur easily at open connectors or between the electrodes of the exposure chamber. These sparks will probably not be destructive but they will prevent proper application of the pulses to the sample. On the other hand, it is convenient to mention that for solid dielectrics even a single breakdown event can severely degrade permanently the insulating capabilities of the material.

3. Monitoring of an ultra short electric signal

3.1 Choice of suitable probes

As pointed above, it is advisable to capture and observe the signals that are actually applied to the exposure chamber. Besides the voltage signal, it can also be convenient to monitor the current that flows through the sample.

The first stage in the acquisition chain consists of the so-called *probes*. A *high-voltage probe* scales down the voltage to levels tolerable by the next stage in the acquisition chain (e.g. a 50 Ω oscilloscope input typically tolerates voltage amplitudes of about 1V) whereas a current probe transforms the current signal into a voltage signal. High-voltage probes are usually based on resistive voltage dividers and high-current probes are generally based on the Hall effect. The specific features of the nsPEFs (high voltage, high current and high bandwidth) impose some serious design constraints for the probes and, as consequence, only a handful of suppliers commercialize suitable probes. Probes useful for monitoring nsPEFs signals are typically employed in applications that involve similar signal features (e.g. Ultra Large Band Radar and plasma generation)

A fundamental limitation of high-voltage probes and current probes is their bandwidth. Typically these probes behave as first-order low-pass filters and their cut-off frequency will determine to a large extent the fidelity of the whole acquisition system. For

instance, the simulations depicted in figure 8 show the response to a 16 ns pulse (including 3 ns + 3 ns rise and fall times) when three voltage probes with different cut-off frequencies are employed: 0.1 GHz, 1 GHz and 10 GHz. As it can be noticed, a voltage probe with a cut-off frequency of 0.1 GHz (trace b) would not only dramatically distort the shape of the original signal but it would also yield an underestimation of the pulse amplitude (70 V instead of 100 V).

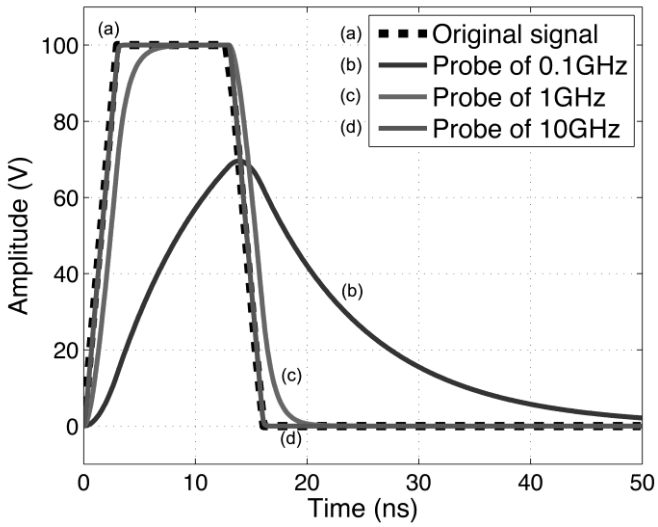

Fig 8 – Time behavior of voltage probes with different cut-off frequencies. Responses (traces b,c and d) have been obtained from SPICE simulations (MacSpice) under the assumption that probes behave as first-order low-pass filters. The simulated original signal (trace a) has an amplitude of 100 V and a duration of 16 ns (including 3 ns + 3ns rise and fall times).

As an alternative to high-voltage probes it is possible to employ *tap-offs*, also known as *power dividers* or *splitters*, inserted in the transmission line. These components are particularly interesting as they allow a direct visualization of the reflections.

3.2 Monitoring devices

Once the high-voltage and current signals have been transformed into low-voltage signals, it is required to capture them and to digitalize them before proceeding to the subsequent monitoring stages (e.g. storage, parameterization and visualization). Different solutions can be adopted in order to perform all the required steps but, in terms of convenience, modern digital oscilloscopes probably outperform all other approaches. Digital oscilloscopes integrate signal acquisition elements together with visualization elements (i.e. display), data storage and parameterization mathematical tools (e.g. automatic quantification of pulse amplitude and width).

The particular features of the nsPEFs signals impose at least two specific characteristics of the monitoring system: 1) large acquisition bandwidth and 2) large memory.

Signal acquisition bandwidth is largely determined by the sampling rate of the analog to digital converter (ADC) embedded within the acquisition system. The Nyquist-Shannon theorem states that it is sufficient to sample at a rate twice higher than the bandwidth of the input signal in order to be able to reconstruct accurately the original waveform. However, oversampling, that is, digitalizing the signal at a higher frequency than twice the bandwidth of the signal being sampled, is commonly performed in signal acquisition systems as it provides some advantages in terms of noise cancellation and facilitates the design of the system. As a matter of fact, digital oscilloscopes generally have sampling rates well above three times the maximum input bandwidth.

A second important feature, especially in case of acquisition of long trains of pulses, is the memory available for the storage of the acquired data. A single 10 ns pulse sampled at 50 GS/s will only require 500 points of memory. However, a single pause of 100 ms between two pulses in a train of pulses (i.e. pulse repetition frequency of 10 Hz) will fill 5×10^9 points of memory which is well above the *memory depth* of current scopes. Fortunately, current high-performance oscilloscopes include a memory segmentation function that allows to record all the "interesting" points whereas the "dull" ones are disregarded: when a pulse is detected (i.e. oscilloscope *trigger*), only a limited number of samples before and after the trigger is recorded so that only the time segments corresponding to the pulses are recorded sequentially in memory. Later on, all the useful information concerning the applied pulses (e.g. amplitude, duration, rise and fall times) can be assessed.

4. Side effects of the application of pulsed electric fields

Administration of pulsed electric fields to biological samples can be accompanied by phenomena not related to the direct effects of the electric fields on biological structures and their constituents. These phenomena, which could be labeled as *interfering phenomena*, must be taken into account and, if possible, avoided in order to simplify the interpretation of the experimental results. Phenomena such as cell electrodeformation (due to Maxwell stress) or ionization of macromolecules should not be included within this category as they are in fact a direct consequence of the pulses on the constituents of the biological sample.

Here we briefly introduce and discuss two groups of *interfering phenomena* caused by application of high field pulses: 1) thermal effects and 2) electrochemical effects. Our description of both families of phenomena is focused on nsPEFs but most of what is said here can be applied also to pulses employed in conventional electroporation.

4.1 Thermal effects

Electrical power is dissipated as heat at any conductor. This phenomenon is known as *Joule heating* but it is also referred to as *ohmic heating* or *resistive heating* because of its relationship with Ohm's law ($V=IR$):

$$P_{dissipated} = V I = I^2 R = \frac{V^2}{R} = V^2 G$$

where $P_{dissipated}$ is the total amount of heat power generated in the whole conductor (expressed in watts, [W]), V is the applied voltage (volts, [V]), I is the current that flows through the conductor (amperes, [A]), R is the resistance of the conductor (ohms, [Ω]) and G is the conductance of the conductor (inverse of the resistance, expressed in siemens, [S]).

The above equation is intended for two-terminal components (e.g. a piece of wire). For infinitesimal volumes the Ohm's law can be expressed as:

$$\rho = \frac{|\mathbf{E}|}{|\mathbf{J}|}$$

where ρ is the resistivity of the material (ohms×meter,[Ω.m]), $|\mathbf{E}|$ is the local magnitude of the electric field ([V/m]) and $|\mathbf{J}|$ is the magnitude of the current density ([A/m^2]). And now it is possible to write down an expression for the dissipated power due to Joule heating in an unitary volume ($p_{dissipated}$, expressed in W/m^3):

$$p_{dissipated} = |\mathbf{E}||\mathbf{J}| = \frac{|\mathbf{E}|^2}{\rho} = \sigma |\mathbf{E}|^2$$

where σ is the conductivity of the material (inverse of ρ, [S/m]).

If it is assumed that no heat exchange occurs within the conductive material and between the material and its environment (i.e. the worst case scenario if sample heating is

undesirable), then the increase in temperature at each sample point (ΔT) can be easily calculated as:

$$\Delta T = \frac{U_{heat}}{c\,d} = \frac{\sigma |\mathbf{E}|^2 t}{c\,d}$$

where t is the time ([s]), U_{heat} is the applied thermal energy (= power × time, expressed in joules, [J]=[W.s]), c is the specific heat capacity of the material (joules/(grams×kelvin), [J/(g.K)]) and d is the mass density of the material ([g/m^3]).

If a single 10 ns pulse of 1 MV/m (10 kV/cm) is applied to a cell suspension in a highly conductive medium (σ=1.5 S/m), the maximum temperature increase that can be expected is only 0.0036 K (c_{water} = 4.184 J/(g.K), $d_{\text{water}} = 0.997\times10^6$ g/m^3), which is negligible under biological experimental conditions. On the other hand, if longer or larger pulses are considered then the temperature jumps can start to be significant. For instance, a single pulse of 5 MV/m and 50 ns would produce a temperature rise of about 0.45 degrees which is probably still too low to cause observable biological effects; particularly taking into account that such temperature increase will only last for a few seconds or fractions of a second in actual setups in which heat dissipates. However, it must be noticed that pulses are commonly applied at repetition frequencies of 1 Hz or higher and, in these cases, temperature can build up if heat does not dissipate rapidly enough. In such cases it is highly advisable to perform thermal measurements (e.g. by means of fiber optic thermal sensors or infrared cameras, which are both fast and free of pulse interference) or to perform numerical thermal modeling of the system (Davalos *et al.* 2005).

The maximum tolerable temperature increase will depend on the experimental conditions and on the objectives of each biological study. As stated by Diller et al. (Diller *et al.* 1999), damage to biological structures resulting from elevated temperatures is very sensitive to the value of the highest temperature that is reached and less so to the time of exposure, but, of course, both factors are important. Nevertheless, although some models have been implemented to describe such double dependency (Diller *et al.* 1999), and have been applied for electroporation (Maor *et al.* 2008), until now most studies in conventional electroporation and in the nsPEF field only consider a maximum value for the temperature increase as the criterion for tolerability. In particular, researchers in the nsPEF field consider that temperature rises of about some tenths of kelvin (Schoenbach *et al.* 2001, Vernier *et al.* 2004) or of a few kelvins (Deng *et al.* 2003, Nuccitelli *et al.* 2006) are perfectly tolerable in their studies.

It must be noted that Joule heating depends on the square of the electric field magnitude. This fact implies that field distribution heterogeneities will have a significant impact on heating. For instance, high electric fields around the electrodes due to the edge effect may cause local thermal burns after nsPEFs administration in the same way that has been observed in conventional tissue electroporation (Edd *et al.* 2006). Moreover, Vernier et al. hypothesized that field distribution heterogeneities at cell or sub-cellular level could cause thermal differences at microscopic level, but those were not noticed in their study (Vernier *et al.* 2004).

Temperature plays an important role in ionic conductance: viscosity of the solvent decreases as temperature rises, increasing ion mobility and, consequently, increasing electrical conductivity. Although such dependence is not very significant (for most aqueous ionic solutions the temperature dependence of conductivity is about + 2 %/K) this phenomenon can in turn have a slight effect on the temperature: as temperature increases due to Joule heating, conductivity increases and therefore Joule heating further increases which accelerates temperature climb.

Finally, we want to point out another temperature-related phenomenon that may have some biological significance: water thermal expansion. When liquid water is heated, its volume increases and, if such volume increase is confined or cannot disperse sufficiently rapidly, as it happens in the case of short thermal bursts, then pressure increases according to the equation:

$$\Delta P = \frac{\alpha}{\beta}\Delta T$$

where ΔP is the resulting pressure increase, α is the thermal expansion coefficient of water (207×10^{-6} K^{-1}), β is the compressibility coefficient of water (4.6×10^{-4} Pa^{-1}) and ΔT is the applied temperature increase. This sudden increase in pressure may have some effect by itself at the location where it is created but it can also affect distant locations as it causes a shockwave that propagates. In fact, this phenomenon has been proposed as a mechanism to generate shockwaves for lithotripsy treatments as an alternative to underwater sparks (US patent 6,383,152 B1). Nevertheless, it does not seem very plausible that this phenomenon could have significant biological consequences. A sudden increase in temperature of 0.5 degrees would imply an increase in pressure of about 225 kPa (2.2 atm). This figure may seem important but in fact is almost negligible taking into account that lithotripsy shockwaves have pressures of about 100 atm and are only effective on hard materials (e.g. kidney stones) and not on soft tissues.

4.2 Electrochemical effects

When DC currents are forced to flow through the interface between an electronic conductor (e.g. a metal) and an ionic conductor (e.g. biological media), oxidation and reduction chemical reactions ("redox" reactions) occur which involve the molecules of the metal (electrode) and those of the ionic media (electrolyte) in a process called electrolysis. Some of the resulting chemical species liberated into the media can interfere with the biological processes up to the point of compromising cell viability. As a matter of fact, at present, electrochemical reactions are intentionally caused with low level currents applied through metallic needles for the ablation of solid tumors in a procedure called electrochemical treatment (EChT) (Nilsson *et al.* 2000).

In comparison to Joule heating, electrochemical effects are fundamentally accumulative: the chemical species created by electrolysis will accumulate pulse after pulse; although some molecules will finally escape as gas or will recombine with molecules in the media to form neutral species.

The main reactions that are believed to occur in biological samples when inert electrodes (e.g. platinum) are employed are (Nilsson *et al.* 2000, Saulis *et al.* 2005):

1) $2H_2O + 2e^- \Rightarrow H_2$ (gas) $+ 2OH^-$ at the cathode.
2) $2H_2O \Rightarrow O_2$ (gas) $+ 4H^+ + 4e^-$ at the anode.
3) $2Cl^- \Rightarrow Cl_2$ (gas) $+ 2e^-$ also at the anode.

Furthermore, if instead of inert electrodes, electrochemically soluble electrodes (e.g. copper, aluminum or stainless steel) are employed, then other oxidation reactions that release metallic ions can also occur at the anode (Kotnik *et al.* 2001b), such as (Saulis *et al.* 2005):

4) $2Al \Rightarrow 2Al^{+3} + 6e^-$

The biological significance of each one of the above reactions and their resulting species is still a matter of debate. Nevertheless, it is believed that H^+ production at the anode (i.e. pH decrease) is particularly important in EChT (Nilson *et al.* 2000) whereas release of Al^+ ions has been found to alter Ca^{2+} homeostasis in cell cultures (Loomis-Husselbee *et al.* 1991).

Faraday's laws of electrolysis indicate that the amount of substance (M), measured in moles (i.e. number of molecules), produced by the above electrochemical reactions will be

proportional to the total electric charge injected by the external source (Q, measured in coulombs, [C]):

$$M \propto Q = \int_{-\infty}^{t} I(t)dt$$

or, for a constant current pulse (I) with Δt duration,

$$M \propto Q = I\,\Delta t$$

Therefore, if it is assumed that electrochemically generated species freely diffuse through the whole sample, it seems reasonable to specify dose for electrochemical treatments as amount of charge per unit of volume ([C/m^3]). In (Yen *et al.* 1999) it is reported that charge to volume ratios as low as 0.3 C/ml (3×10^5 C/m^3) have an impact on cell growth. That figure can be put in the perspective of the nsPEFs with the following example: a single 1 MV/m pulse of 10 ns applied in a cuvette with an electrode area of 1 cm^2 and an electrode separation of 1 mm (i.e. volume= 1×10^{-7} m^3 = 0.1 ml) would produce a charge of approximately 15 μC/ml assuming that the medium had a conductivity of 1.5 S/m. Therefore, in order to reach the 0.3 C/ml dose, 20,000 pulses would be required, which is much higher than the number of pulses that researchers usually apply in the nsPEF field. On the other hand, since the amount of charge is proportional both to the pulse duration and to the current, a single 5 MV/m pulse of 50 ns applied to the same setup would produce a charge of 375 μC/ml. In this case, for reaching the 0.3 C/ml dose 800 pulses would be required, which, although is still higher than the number of pulses usually applied, comes closer to actual experimental conditions. Furthermore, two facts must be noted here for precaution: 1) the 0.3 C/ml dose was obtained under specific experimental conditions and quite probably the dose for other conditions and other biological effects is significantly lower; and 2) at higher voltages the kinetics of the electrochemical reactions may be significantly different and other chemical species could be produced. In other words, currently there is the need for experimental studies in which the dose to avoid electrochemical effects is obtained for conditions equivalent to those used with nsPEFs.

It is interesting to note that Vijh (Vijh *et al.* 2004) points out hydrogen cavitation at the cathode as a possible cause of erosive damage to tissues in electrochemical treatments. As far as we know, this hypothetical source of damage is not mentioned by other authors in the field, which is not surprising considering the low rate at which hydrogen is generated in standard electrochemical treatments. However, with nanosecond pulses of high intensity this phenomenon appears more plausible because the amount of gas suddenly created is quite significant. Moreover, the gas bubbles created at the anode (O_2 and Cl_2) and the cathode (H_2) may not withstand the magnitude of the nsPEF and dielectric rupture (i.e. sparks) may occur accompanied by pressure shockwaves and flashes of light. In this case the pressure of the shockwaves could be higher than that of those caused by the water thermal expansion phenomenon. Further research is required in this area.

Conclusion

A reliable nsPEF generator is a necessary but not sufficient prerequisite for reproducible experimentation in the field of nsPEFs delivery to biological samples. Here our aim has been to point out different aspects that can have a very significant impact on the experimental conditions. Our own experience tells us that those aspects can be easily overlooked, particularly by those research teams more focused on the biological aspects of nsPEFs delivery or those that come from the conventional electroporation field. Hence the present chapter should be taken as a caution message for those researchers interested in entering this field.

In this chapter we have described first how the propagation phenomenon and particularly one of its associated phenomena, the reflection phenomenon, have a very relevant

impact on the pulse field that is actually applied to the sample. Then we have explained that, up to a point, it is possible to control those reflections by matching the impedance of the exposure cell. Nevertheless, due to the uncertainties of this impedance matching process, we consider that voltage and current monitoring systems are highly advisable and we have given some indications about the use of these systems and their limitations. Furthermore, since high-voltage is a fundamental attribute of nsPEF signals, we have provided some details on the electrical breakdown phenomenon.

Finally, we have discussed two groups of side effects of the application of nsPEFs: electrochemical and thermal effects. Actually, both families of phenomena are also present in the case of conventional electroporation. The extremely short duration of the nsPEFs does not necessarily avoid the problems related to the electrochemical formation of chemical species at the electrode-sample interface. Temperature rise because of the Joule effect will be particularly significant if the nsPEF application comprises a train of pulses at a high repetition frequency.

NsPEF can be an extraordinary tool for intracellular electromanipulation. The use of nsPEFs may raise many hopes in terms of improvement of our knowledge in cell biology and cell functioning, as well as in terms of development of new biotechnological and biomedical applications. The future will confirm these hopes or prove them wrong. In any case, only well-controlled experimental conditions will result in robust and reproducible biological effects and in their translation into interesting applications.

Acknowledgements

The work of the authors is supported by grants of the CNRS, Institut Gustave-Roussy, Univerité Paris-Sud, EU 6th FP (CLINIGENE - FP6, LSH-2004-018933), INCA (Institut National of Cancer, France - contract number 07/3D1616/Doc-54-3/NG-NC), DGA/D4S/MRIS (contract number 06 34 017) and French National Agency (ANR) through Nanoscience and Nanotechnology Program (Nanopulsebiochip n° ANR-08-NANO-024-01)

References

Beddow, AJ. Brignell, JE. 1966. Nanosecond breakdown time lags in a dielectric liquid. *Electronics Letters* 2: 142-143.

Crowley, J.M. 1973. Electrical breakdown of bimolecular lipid membranes as an electromechanical instability, *Biophys. J.*,13: 711-724.

Davalos, R.V. Mir, L.M. Rubinsky, B. 2005. Tissue ablation with irreversible electroporation. *Annals of Biomedical Engineering* 33: 223-231.

Deng, J. Schoenbach, KH. Buescher, ES. Hair, PS. Fox, PM. Beebe, SJ. 2003. The effects of intense submicrosecond electrical pulses on cells. *Biophys. J.* 84: 2709-2714.

Diller, K.R. Pearce, J.A. 1999. Issues in modeling thermal alterations in tissues. *Annals of the New York Academy of Sciences* 888: 153-164.

Edd, J.F. Horowitz, L. Davalos, R.V. Mir, L.M. Rubinsky, B. 2006. In vivo results of a new focal tissue ablation technique: irreversible electroporation. *IEEE Trans. Bio-Med. Eng.* 53: 1409-1415.

Garon, EB. Saweer, D. Vernier, PT. *et al.* 2007. *In vitro* and *in vivo* evaluation and a case report of intense nanosecond pulsed electric field as a local therapy for human malignancies. *Int. J. Cancer* 121: 675-682.

Hall, E.H. Schoenbach, K.H. Beebe, S.J. 2007. Nanosecond pulsed electric fields have differential effects on cells in the S-Phase. DNA and Cell Bio. 26: 160-171.

Kolb, JF. Kono, S. Schoenbach, KH. 2006. Nanosecond pulsed electric field generators for the study of subcellular effects. *Bioelectromagnetics* 27: 172-187.

Kotnik, T. Mir, L.M. Fisar, K. Puc, M. Miklavcic, D. 2001a. Cell membrane electropermeabilization by symmetrical bipolar rectangular pulses. Part I. Increased efficiency of permeabilization. *Bioelectrochemistry.* 54: 83-90.

Kotnik, T. Miklavcic, D. Mir, L.M. 2001b. Cell membrane electropermeabilization by symmetrical bipolar rectangular pulses. Part II. Reduced electrolytic contamination. *Bioelectrochemistry* 54: 91-95.

Loomis-Husselbee, J.W. Cullen, P.J. Irvine, R.F. Dawson, A.P. 1991. Electroporation can cause artefacts due to solubilization of cations from the electrode plates. Aluminum ions enhance conversion of inositol 1,3,4,5-tetrakisphosphate into inositol 1,4,5-trisphosphate in electroporated L1210 cells. *Biochem. J.* 277: 883-885.

Maor, E. Ivorra, A. Rubinsky, B. 2008. Intravascular irreversible electroporation: theoretical and experimental feasibility study. *Conference Proceedings: Annual International Conference of the IEEE Engineering in Medicine and Biology Society. IEEE Engineering in Medicine and Biology Society. Conference* 2008: 2051-2054.

Nilsson, E. Von Euler, H. Berendson, J. *et al.* 2000. Electrochemical treatment of tumours. *Bioelectrochemistry* 51: 1-11.

Nuccitelli, R. Pliquett, U. Chen, X. *et al.* 2006 Nanosecond pulsed electric fields cause melanomas to self-destruct. *Biochem. Biophys. Res. Comm.* 343: 351-360.

Pakhomov, A.G. Kolb, J.F. White, J.A. Joshi, R.P. Xiao, S. Schoenbach, K.H. 2007. Long-lasting plasma membrane permeabilization in mammalian cells by nanosecond pulsed electric field (nsPEF). *Bioelectromagnetics* 28:655-663.

Saulis, G. Lape, R. Praneviciūte, R. Mickevicius, D. 2005. Changes of the solution pH due to exposure by high-voltage electric pulses. *Bioelectrochemistry* 67: 101-108.

Schoenbach, K.H. Beebe, S.J. Buescher, E.S. 2001. Intracellular effect of ultrashort electrical pulses," *Bioelectromag*. 22: 440-448.

Sun, Y. Vernier, PT. Bebrend, M. Marcu, L. Gundersen, MA. 2005. Electrode microchamber for noninvasive perturbation of mammalian cells with nanosecond pulsed electric fields. *IEEE Trans. Nanobioscience*. 4: 277-283.

Vernier, P.T. Sun, Y. Marcu, L. Craft, C.M. Gundersen, M.A. 2004. Nanoelectropulse-induced phosphatidylserine translocation. *Biophys. J.* 86: 4040-4048.

Vijh, A.K. 2004. Electrochemical treatment (ECT) of cancerous tumours: necrosis involving hydrogen cavitation, chlorine bleaching, pH changes, electroosmosis. *Int. J. Hydrogen Energy*. 29: 663-665.

Yen, Y. Li, J.R. Zhou, B.S. Rojas, F. Yu, J. Chou, C.K. 1999. Electrochemical treatment of human KB cells in vitro. *Bioelectromagnetics* 20: 34-41.